



Deposited via The University of Leeds.

White Rose Research Online URL for this paper:

<https://eprints.whiterose.ac.uk/id/eprint/147425/>

Version: Accepted Version

Proceedings Paper:

Abdelwahab, MM and Tsavdaridis, KD (2019) Optimised 3D Printed Metallic Node-Connections for Reticulated Structures. In: Lam, D, Dai, X, Yang, T and Zhou, K, (eds.) Proceedings of the 9th International Conference on Steel and Aluminium Structures (ICSAS19). 9th International Conference on Steel and Aluminium Structures (ICSAS19), 03-05 Jul 2019, Bradford, UK. Independent Publishing Network, pp. 423-434. ISBN: 978-1-78972-197-3. ISSN: 0141-0296.

This is an author produced version of a paper published in Proceedings of the 9th International Conference on Steel and Aluminium Structures (ICSAS19).

Reuse

Items deposited in White Rose Research Online are protected by copyright, with all rights reserved unless indicated otherwise. They may be downloaded and/or printed for private study, or other acts as permitted by national copyright laws. The publisher or other rights holders may allow further reproduction and re-use of the full text version. This is indicated by the licence information on the White Rose Research Online record for the item.

Takedown

If you consider content in White Rose Research Online to be in breach of UK law, please notify us by emailing eprints@whiterose.ac.uk including the URL of the record and the reason for the withdrawal request.

OPTIMISED 3D-PRINTED METALLIC NODE-CONNECTIONS FOR RETICULATED STRUCTURES

Moustafa Mahmoud ABDELWAHAB^a and Konstantinos Daniel TSAVDARIDIS^b

^a Undergraduate Student, School of Civil Engineering, University of Leeds, LS2 9JT, Leeds, UK
Emails: fy15mma@leeds.ac.uk, helalsafa646@yahoo.com

^b Associate Professor of Structural Engineering, School of Civil Engineering, University of Leeds, LS2 9JT,
Leeds, UK
Emails: K.Tsavidaridis@leeds.ac.uk

Keywords: Structural Topology Optimisation; Additive Manufacturing; Structural Connections; 3D Printing; Reticulated Structures; Advanced Manufacturing.

Abstract. *Structural Topology Optimisation (STO) is a prevalent optimisation technique used nowadays to reach highly complex and efficient designs (weight-to-stiffness ratio) unable to achieve otherwise. Additive Manufacturing (AM) is a developing manufacturing process which overcomes many of the manufacturing limitations and realises highly optimised products through a layer-based fabrication process. Recent research on reticulated structures proposed using STO and 3D printing to design and fabricate alternative bespoke complex connection designs which have shown its significance through obtaining substantial weight reductions for the same structural capacity. This paper builds on previous research through optimising a single-layer S355 traditional node-connection under four loading cases, producing a state-of-the-art optimised connection design capable of withstanding the four loading cases considered and comparing the results to the traditional ones. In all loading cases, optimised shapes with 46.90% weight reduction were obtained with varying stress levels. A selection of the highly bespoke designs were 3D printed as a proof of concept for the applicability of AM.*

1) INTRODUCTION

Reticulated roofs are highly versatile structures and are commonly used in the construction industry. Otherwise known as spatial structures, such structures achieve a cost-effective span-weight ratio for roof constructions and manage to reduce the number of intermediate column supports required. Their numerous applications range from stadiums to warehouses to aircraft hangers [1]. Fundamental changes and improvements have been undertaken on these structures over the years to increase their structural capacity, simplify their fabrication and erection techniques, and improve the performance of their node-connections. However, the fundamental worldwide shift in architectural perspectives from modular and repetitive to free-form and unique is imposing critical challenges, most of which are related to the connections of such structural systems.

1.1) Background and critical review

Previous attempts by researchers aimed at exploring the potential of using Structural Topology Optimisation (STO) as a mean of creating bespoke node-connection designs which can accommodate the variability of the tie member directions and angles in free-form shapes [2, 3, 4]. The node-connection designs achieved had the major benefit of attaining significant weight reductions which on a large scale can result in an improvement to the overall structural performance. Such node-connection designs were observed to have geometrical complexities and curvature patterns which were highly challenging to construct using traditional fabrication methods such as milling or casting, nor using subtractive manufacturing. Consequently, additive manufacturing was proposed as a suitable manufacturing alternative.

1.2) Additive manufacturing

Additive Manufacturing (AM), commonly known as 3D printing, is a layer-based fabrication process which creates a physical model through depositing and joining thin layers of a material together based on a 3D computer model [5]. Research institutions and the industry worldwide are investing in 3D printing due to its high precision and minimal fabrication limitations when compared to traditional manufacturing. The technology has seen drastic developments since its introduction in the 90s through improving the fabrication process and allowing fabrication using a wider range of materials which include metals, ceramics, and polymers [6]. From the literature, it is apparent that manufacturing industries related to aerospace, automotive, and medical (prosthetics) have strong interest in attaining the full potential of 3D printing, unlike the construction industry which seems to be moving at a much slower pace for a number of reasons (size of printed elements, high load bearing, long lifespan, etc.) [6]. This paper aims to support the limited research in bridging the gap between 3D printing and its application in the construction industry through the structural testing of 3D printed node-connections for reticulated structures.

1.3) Research objectives

This paper builds upon previous research attempts through optimising a single-layer S355 node-connection against four loading cases and observing the optimisation results. A state-of-the-art optimised node-connection design referred to as “Connection B” was achieved following STO and finite element (FE) analysis, which is capable of withstanding each of the four loading conditions considered. The optimisation of all the node-connection in this research was undertaken to achieve 53.10% of the weight of the traditional node-connection. At last, the structural behaviour of the traditional connection was compared to all the optimised connections and the bespoke “Connection B”.

2) SELECTION CRITERIA OF THE CONNECTION DESIGN

A comprehensive study was undertaken to identify state-of-the-art node-connections commonly used in the industry and choose the potential connection which would represent our control sample. Simplicity was a key part of the research, therefore, a list of questions has been prepared which helped decide upon the joint type which is likely to be the simplest to model and optimise. Yet, yield significant weight reductions which then translate to reduced carbon emissions and a more sustainable design. The questions considered include the following:

- What is the total volume occupied by the connection?
- What is the material percentage in the total volume occupied by the connection?
- How simple would the connection be to create, model, and test?
- How simple would the connection be to predict its behaviour upon modelling?
- Does the connection need to have any internal bolting or welding?
- How are the tie members attached to the connection?
- How much commercial knowledge is available to judge upon the typical loading capacity and dimensions of the connection?

3) TRADITIONAL NODE-CONNECTION DESIGN CONCEPT

Based on the above questions and after reviewing numerous connection types, the Splice Node-Connection “POLO-1” shown in figure 1 has been chosen as it represented the ideal candidate for this research [7, 8]. The applications for this connection range from geodesic domes to reticulated structures. The connection consists of a central thick RHS core with several splice plates welded to it. The tie members attached to this connection are fabricated with a fork-shaped ending which fits in between the plates of the connection. The central RHS region provided the large volume needed for the freedom of shape formation by the optimisation algorithm and achieved the design simplicity and ease of behaviour predictability sought. Furthermore, eliminating any bolting from the central area and keeping the bolting to the splice steel plates provides further simplicity in the modelling.



Figure 1: Splice node-connection “POLO-1” [9, 10].

3.1) The design anatomy

After the structural modifications to be discussed later in the paper have been undertaken, the structure of the connection has been divided into two regions, the design domain and non-design domain. The design domain region as shown in red in figure 2 below is the region which was optimised by the software. The non-design domain region which was not optimised by the software consists of the connecting splice steel plates indicated in grey and the semi-cylindrical members indicated in green, which were added to allow for improved stress flow and shape development within the design domain area. Similar model division has been undertaken in the traditional connection design to ensure a fair comparison between the stress and strain level of the results of both the traditional and optimised connections.

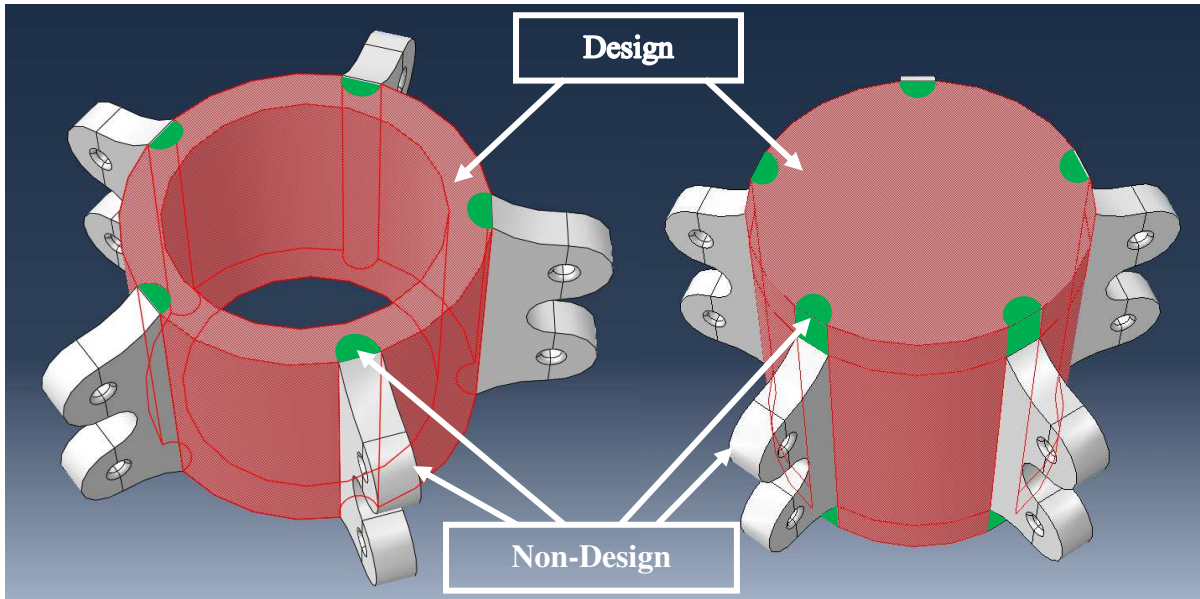


Figure 2: Design anatomy of the traditional node-connection and “Connection A”.

3.2) Loading cases considered

In total, four loading cases were considered as shown in figure 3, which simulate a spectrum of asymmetrical loading scenarios and provide the variations required in the loading types and magnitudes. Even though this connection type is capable of resisting moments too, axial loads were only used in the optimisation process. The resultant of all the applied loads in each of the loading cases sums up to zero.

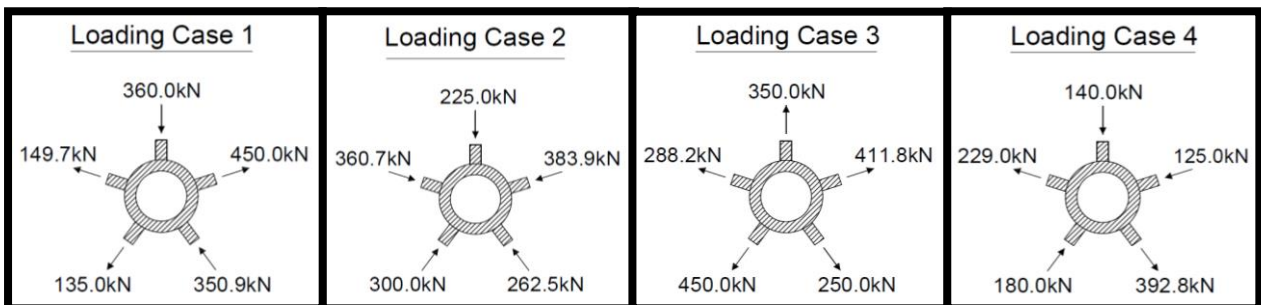


Figure 3: Loading cases applied to the node-connections.

3.3) Methods and tools

Three software packages were employed throughout the various stages of this research. Fusion 360 was the main design tool which was used to create the connection designs and undertake shape improvements. ABAQUS/CAE was used for the FE analysis testing and the STO stages. MeshMixer was then used to post-process and refine the rough and low-quality connection designs extracted from ABAQUS to more printable structures.

4) OPTIMISATION PROCESS

The optimisation process used in this research as shown in figure 4 contains the core elements from the processes established by previous relevant research [11, 12]. Steps 1 and 2 in the design process started by creating the traditional connection model in Fusion 360 and visually optimise its shape [13]. A modified version of the traditional connection shown in step 3 was created with the central volume filled with material. This modified version which is referred to as “Connection A” will be utilised during the optimisation task. “Connection A” was uploaded into ABAQUS, meshed and analysed against the loading cases considered as shown in steps 4 and 5. “Connection A” was then optimised in step 6 at a specified weight percentage against one loading case at a time to obtain the final optimised results after hundreds of heuristic trials. To obtain “Connection B” which was optimised simultaneously against the abovementioned four loading cases, step 6 was re-undertaken with the four loading cases input into the software rather than a single case. In steps 7 and 8, the produced designs were then exported from ABAQUS to MeshMixer for post-processing and smoothing to prepare for 3D printing. Finally, in step 10, the modified traditional connection design was imported into ABAQUS and applied the same conditions, and tested against the aforesaid loading cases in order to act as the control sample in this research.

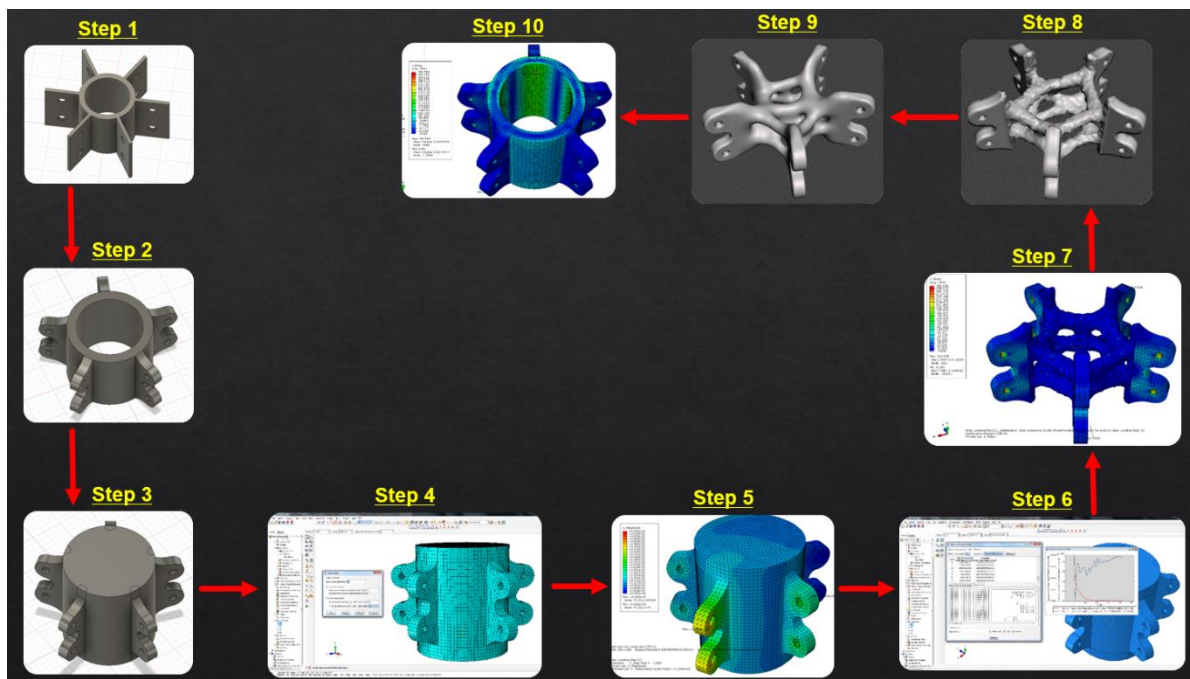


Figure 4: Design process.

4.1) Design modifications

Initial modifications to the design of the splice steel plates were introduced through adding the semi-circular shape shown in figure 5 around the bolt holes in all the considered models and filleting the sharp edges of the holes. Such modifications allowed for a reduction in the overall weight of the connections, allowed for a better stress flow through the structure and utilised the full fabrication potential of AM through introducing complex geometry.

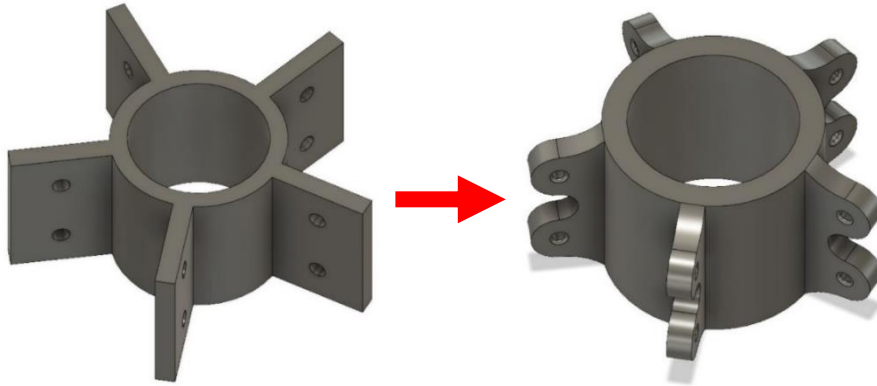


Figure 5: Splice node-connection “POLO-1” before and after design modifications.

4.2) Material properties and permissible stress levels

For all the node-connections in this project, a steel grade of S355 was used to define the material properties, 210 GPa was chosen as the Modulus of Elasticity and 0.3 as the Poisson’s ratio. An early assumption was made regarding the permissible stress levels in the node-connections. A linear-elastic analysis was undertaken, therefore, it was assumed the stress levels in the design-domain region of the connections shall not exceed 355N/mm^2 . The loading cases and percentage weight reduction considered were achieved through trying a number of iterations while monitoring the maximum stress levels observed.

4.3) Meshing

“Connection A” was imported in ABAQUS and the properties were assigned as well as the loads and boundary conditions were applied. The FE meshing of the connection is shown in figure 6. A free meshing technique using quadratic tetrahedron element (Element type: C3D10) was used due to the model’s complex geometry. The mesh size was chosen as 12 and remained constant across all the models undertaken in this research to avoid accuracy-related variations. The number of elements and nodes obtained in the model are 148438 and 212127, respectively.

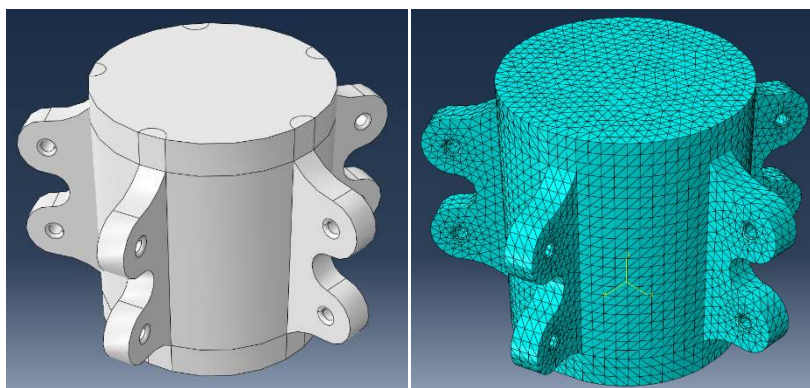


Figure 6: Meshing of “Connection A” for the optimisation.

4.4) Weight percentage

The weight percentage of the traditional connection to be used in the optimisation tasks was taken as 53.10%, which produced optimised designs that consistently remained within the linear elastic range. The few initial loading cases considered when optimising “Connection A” were excluded either due to excessively high stress levels or minimal material formation in local areas. This minimal material formation was later attributed to the low straining caused by low loads which resulted in minimal or no material formation at a particular member or throughout the entire design-domain region. Based on that, loading cases with high enough magnitudes were selected. These loading cases utilised a significant capacity of the splice steel plates and resulted in a reasonable material formation throughout the design-domain region.

4.5) Optimisation approach

Additive Stiffness-based Structural Topology Optimisation process has been adopted in this research which allows the addition of material only in the regions displaying noticeable displacement in the structure. Thus, the design-domain region in “Connection A” has been filled with material as shown in figure 6 to undertake the optimisation task.

Following the model preparation, the design-domain region was defined in ABAQUS and “Minimising the connection volume” of the target volume was introduced as the optimisation objective, while “Minimising the maximum design response values” of the strain energy was taken as the optimisation constraint. For each of the loading cases, an optimised design has been obtained as shown in figures 7, 8, 9 and 10. In order to obtain “Connection B” which is shown in figure 11, the optimisation objective remained the same, while the optimisation constraint was changed to account for the maximum strain value associated with each loading case. The maximum number of cycles allowed in each optimisation trial was taken as 200 cycles, which was proven enough to allow the software to reach the optimal design, achieving the highest stiffness at the target volume specified. The actual number of cycles ranged from 28 to 50.

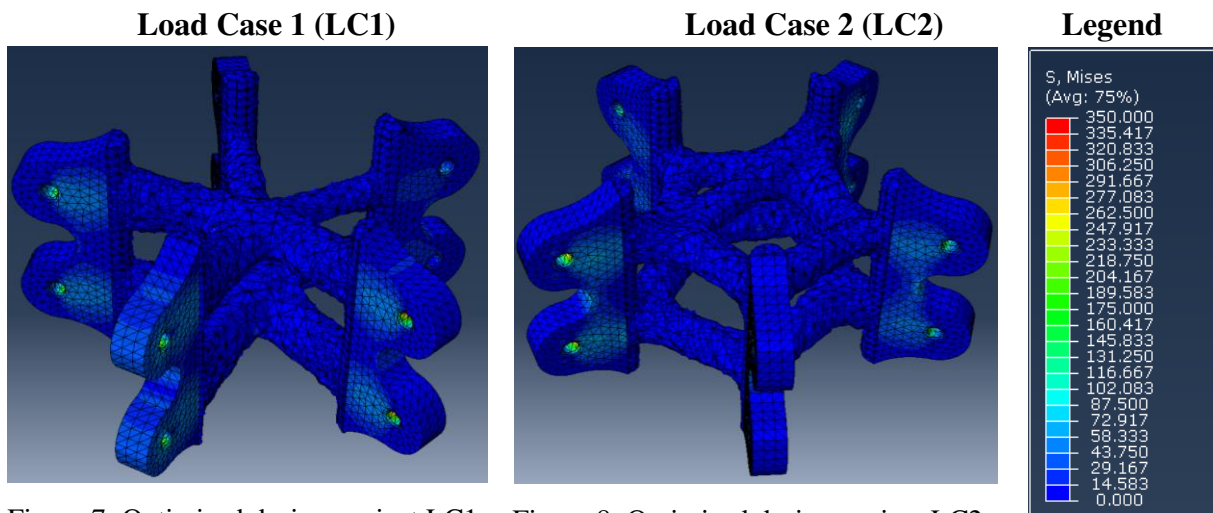


Figure 7: Optimised design against LC1. Figure 8: Optimised design against LC2.

Load Case 3 (LC3)

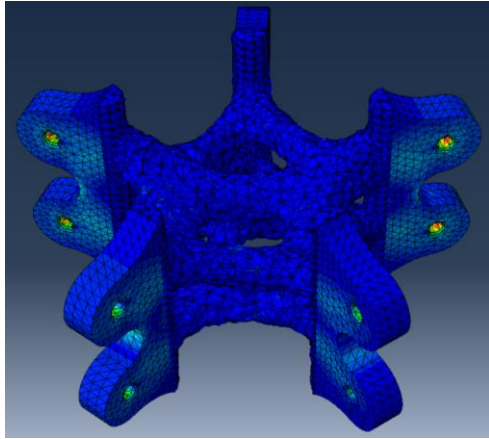


Figure 9: Optimised design against LC3.

Load Case 4 (LC4)

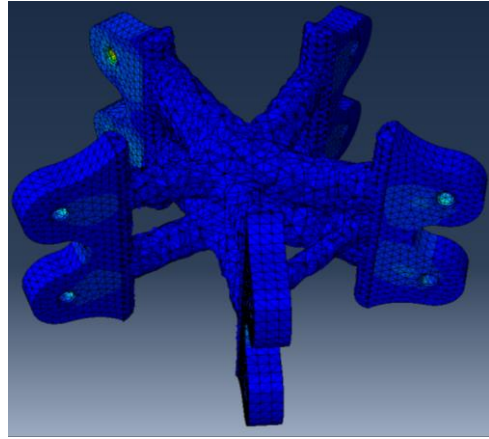


Figure 10: Optimised design against LC4.

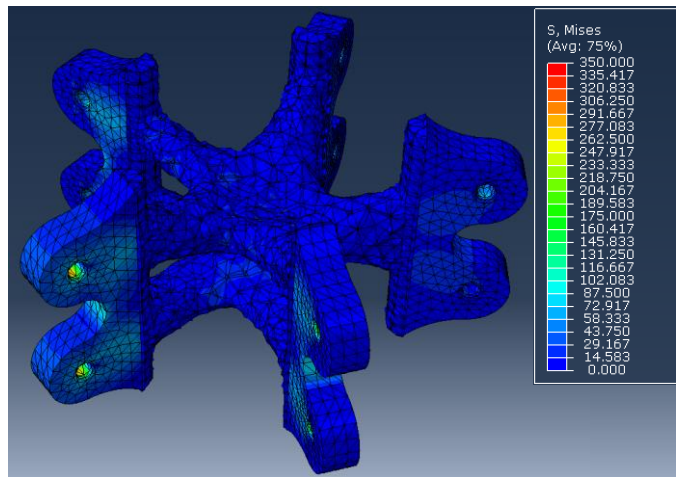


Figure 11: FEA structural testing of “Connection B” against LC1.

4.6) Comparative study

Once all the optimisation work has been undertaken, the same load cases used in the optimisation tasks were applied to the traditional connection, and figure 12 shows the Von Misses stress contour plot of the traditional connection against loading case 1. Identical dimensions, features and meshing technique were used in the traditional connection to avoid accuracy-related variations. Moreover, the stress and strain levels were measured at the design-domain region of the traditional connection to allow for a fair comparison.

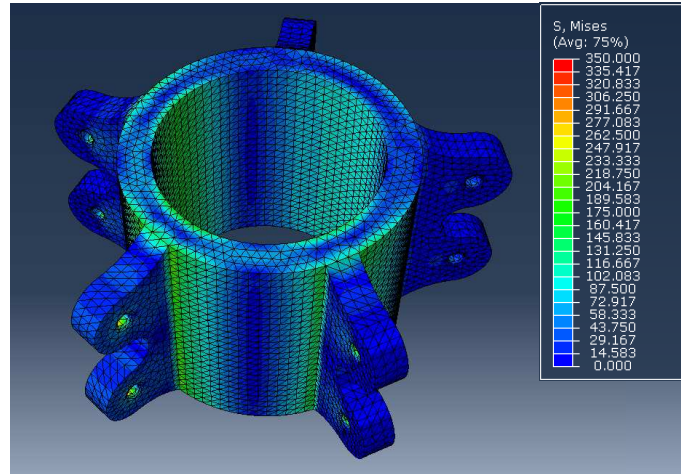


Figure 12: FEA structural testing of the traditional node-connection against LC1.

5) COMPARISON OF RESULTS

Figures 13 and 14 demonstrate a comparison between the recorded stress and strain levels in the design-domain area in the traditional connection, the optimised designs, and “Connection B”. The non-design domain stress and strain levels are not the focus of this research study, therefore, their values were not presented.

In loading cases 2 and 3 which consisted of entirely tensile and compressive loads with different magnitudes acting on each splice plate, the traditional connection displayed the lowest stress levels and significantly low strain levels. As for loading cases 1 and 4 which consisted of a combination of tensile and compressive loads on the splice plates, the optimised models had a better performance with lower stresses than both the traditional connection and “Connection B”, and displayed relatively low strain levels. As “Connection B” was optimised to all of the four loading cases, the ideal shape formed was not specific towards a single loading case, rather, all of them. Therefore, the resulted “Connection B” contains the highest stress levels in three out of four of the cases and some varying strain levels. Generally, more loading cases will have to be considered before a more definite conclusion could be reached regarding the performance of the optimised connections.

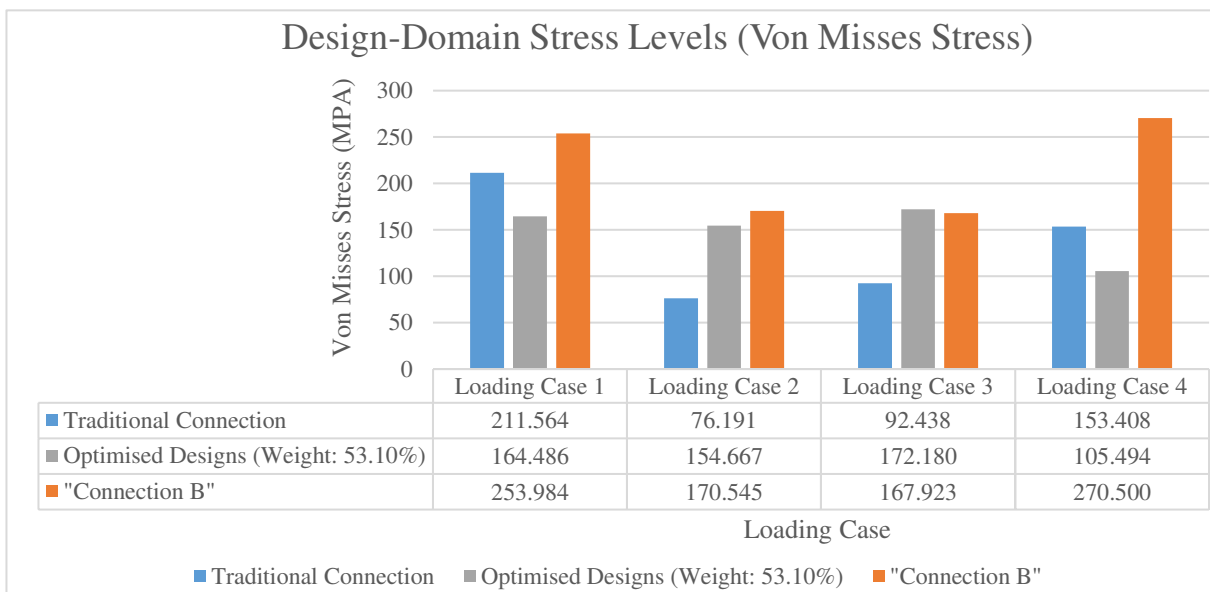


Figure 13: Recorded stress levels.

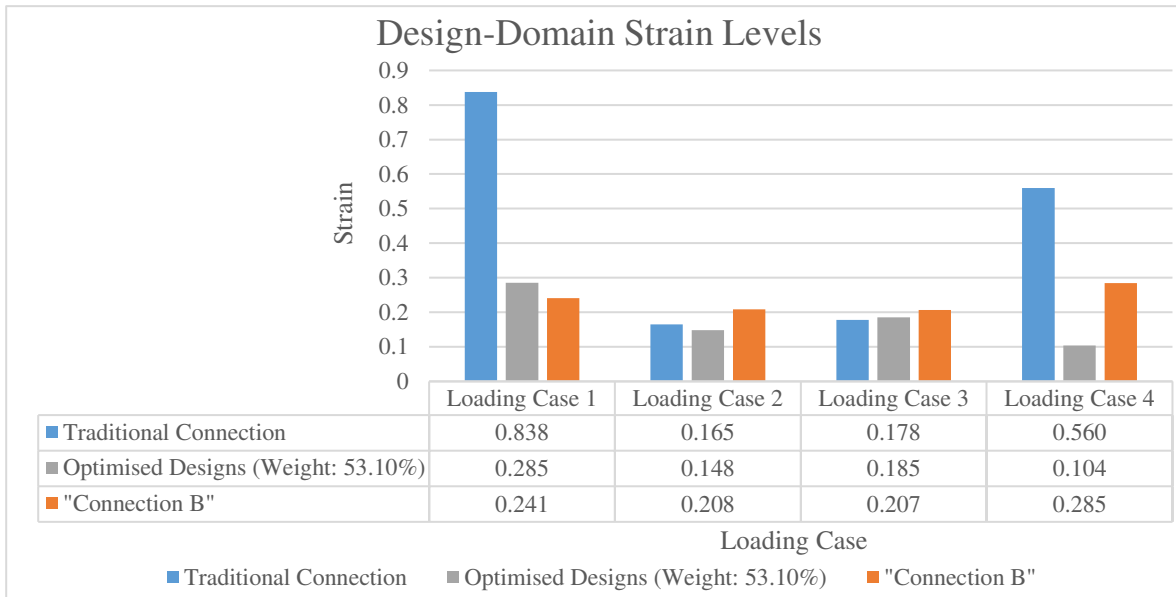


Figure 14: Recorded strain levels.

6) MANUFACTURING PROCESS

The optimised designs extracted from ABAQUS experienced low mesh quality and required further refinement in preparation for 3D printing. In total, four scaled-down optimised designs with bespoke and complex geometries were manufactured. The fabrication of these prototypes showcases the capability of 3D printing in producing intricate shapes and its advantage through eliminating many of the traditional manufacturing constraints.

6.1) Post-processing and preparation for 3D printing

The post-processing steps undertaken on the optimised designs prepared them structurally and geometrically for the 3D printing process. These steps involved creating smoother curves, removing any weak regions likely to develop during the printing, and reducing the number of sacrificial structural supports required. Moreover, the modifications undertaken improved the mesh quality to allow for a more accurate fabrication as shown in figure 15 below. Care was taken while using MeshMixer to maintain the original design-domain geometry of the connections, while allowing for improved overall curvatures in the shape.

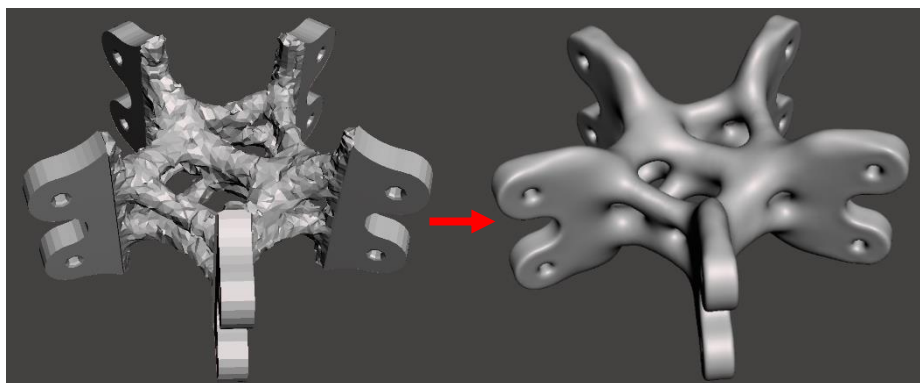


Figure 15: An optimised node-connection before and after post-processing.

6.2) 3D printing and the fabricated designs

Two different materials were used in 3D printing the designs, the first is a metallic alloy formed through a combination of both Steel (60%) and Copper (40%) and was used for three designs which exhibited the highest shape complexity as shown in figure 16 below. The second is a polymer-based material known as “Polyamide”, and it was used for the traditional connection and another complex design established with a Weight Reduction of 53.54%. The designs printed in the metallic alloy were manufactured through the Direct Metal Laser Sintering process, while the Polyamide designs were printed through Jet Fusion Technology.



Figure 16: 3D printed node-connection designs.

7) CONCLUSIONS AND FUTURE RESEARCH

This paper investigates the use of STO and AM on the application of node-connections in reticulated structures. A traditional node-connection is optimised against individual four loading cases at a percentage weight reduction of 46.90%. In addition, an optimised connection design “Connection B” is achieved which is capable of withstanding each of the four loading cases. A comparison of the design-domain stress and strain levels between the traditional connection and the optimised connections is presented in this paper. Finally, a selection of the generated highly bespoke and complex optimised designs has been 3D printed in metal and polyamide.

Ongoing research is focusing on improving the complexity of the node-connection model, validating the results through experimental testing as well as considering a wider range of loading cases in designing “Connection B” and comparing its performance to the traditional connection. Research also focuses on studying the cost-effectiveness and environmental impact of the 3D printed connections.

8) ACKNOWLEDGEMENTS

The authors of this paper would like to thank Lord Laidlaw for the generous financial contribution and the Leadership training provided by the Laidlaw Undergraduate Research and Leadership Scholarship programme. This project and the 3D printing of the node-connections would not have been possible without the Laidlaw Scholarship. The authors would also like to acknowledge the contribution to this project by Dr Osvaldo M. Querin on his guidance on the structural optimisation process.

REFERENCES

- [1] G. Ramaswamy, M. Eekhout, G. Suresh, M. Papadrakakis, Analysis, design and construction of steel space frames, Thomas Telford, London, 2002.
- [2] S. Galjaard, S. Hofman, N. Perry, S. Ren, Optimizing Structural Building Elements in Metal by using Additive Manufacturing. (2015).
- [3] S. Galjaard, S. Hofman, S. Ren, New Opportunities to Optimize Structural Designs in Metal by Using Additive Manufacturing, Advances In Architectural Geometry 2014. (2014) 79-93.
- [4] K. Crolla, N. Williams, M. Muehlbauer, J. Burry, SMARTNODES PAVILION Towards Custom-optimized Nodes Applications in Construction, RMIT Research Repository. (2015) 467-477.
- [5] T. Ngo, A. Kashani, G. Imbalzano, K. Nguyen, D. Hui, Additive manufacturing (3D printing): A review of materials, methods, applications and challenges, Composites Part B: Engineering. 143 (2018) 172-196.
- [6] X. Wang, M. Jiang, Z. Zhou, J. Gou, D. Hui, 3D printing of polymer matrix composites: A review and prospective, Composites Part B: Engineering. 110 (2017) 442-458.
- [7] K. Hwang, Advanced investigations of grid spatial structures considering various connection systems, OPUS - Publication Server of the University of Stuttgart. (2010).
- [8] S. Stephan, J. Sánchez-Alvarez, K. Knebel, Reticulated Structures on Free-Form Surfaces. (2010).
- [9] EA European Architecture, 120 EA-Wood Structures, Pinterest. (2018).
- [10] 2015 Design Biennial Boston, Archdaily. (2015).
- [11] H. Seifi, A. Rezaee Javan, S. Xu, Y. Zhao, Y. Xie, Design optimization and additive manufacturing of nodes in gridshell structures, Engineering Structures. 160 (2018) 161-170.
- [12] H. Seifi, M. Xie, J. O'Donnell, N. Williams, Design and Fabrication of Structural Connections Using Bi-Directional Evolutionary Structural Optimization and Additive Manufacturing, Applied Mechanics And Materials. 846 (2016) 571-576.
- [13] J. O'Donnell, H. Seifi, B. Sitler, N. Williams, K. Crolla, Y. Xie, Smart nodes pavilion: Bi-directional evolutionary structural optimization and additive manufacturing, RMIT Research Repository. (2015) 1-12.